https://doi.org/10.5194/wes-2020-21
Preprint. Discussion started: 11 March 2020

eawe european academy of wind energy
Open Access WIND ENERGY SCIENCE DISCUSSIONS

Field test of an active flap system on a full scale wind turbine

Alejandro Gomez Gonzalez[1], Peder B. Enevoldsen[1], Athanasios Barlas[2], and Helge A. Madsen[2]

[1]Siemens Gamesa Renewable Energy A/S, Brande, DK
[2]Technical University of Denmark DTU, Dept. of Wind Energy, Roskilde, DK

Correspondence: A Gomez (alejandro.gonzalez@siemensgamesa.com)

Abstract.

This article describes a series of validation tests of an active flap system (AFS) on a multi-MW wind turbine. A single blade of a 4 MW turbine with 130m rotor diameter (SWT-4.0-130) is retrofitted in the outer 15-20 m with the AFS. The AFS is controlled remotely with a pneumatic pressure supply system located in the hub of the turbine. The measurements are performed between October 2017 and June 2019 using two different AFS configurations on the blade. A description of the system setup is given, as well as comparisons of measurements and aeroelastic simulations. The measurements quantify the static load control authority of the AFS in atmospheric conditions, providing a preliminary estimate of load impact potential for the concept. The article presents furthermore a new method for the characterization of the load impact of the system and its dynamic response based on a blade-to-blade load comparison.

1 Introduction

Load control and performance optimization of wind turbines using active flap systems have been the subject of numerous studies in the past. It is not within the scope of this paper to give a comprehensive review of the state of the art of active flow control on wind turbines, but to focus solely on the efforts towards active flow control validation at full scale. For an extensive review of the state of the art in smart rotor control, the reader is referred to Barlas (2009), who covers both active control surfaces such as flaps and microtabs, but also other active flow control technologies such as boundary layer control or active twist. Furthermore, the reader is also referred to Pechlivanoglou (2013), who in his dissertation gives a broad overview of different active and passive control technologies for wind turbines as well as comparisons among them, as well as to Johnson (2008) also providing an overview of active load control strategies for wind turbines.

In terms of full scale validation of active flow control on wind turbines, the academic and industrial contributions are scarce. In the decades prior to the modern boom of wind energy, active flow control on wind turbine blades seemed almost natural, as the technology used for the development of turbine blades was driven mainly by know-how transfer from the aeronautical industry. A clear example of this is the design of a 7.3 MW, 122m rotor diameter turbine within the frame of the MOD-5A program in the early 1980's (MOD5A, 1984). In the design of this turbine, which was never commercialized, three independent ailerons, fully integrated in the outboard section of the blades and activated with a hydraulic system, were used both for loads and power control. Nevertheless, the active flow control strategy of the MOD-5A turbine was not the focus at that time, but rather a choice taken at one of the later design stages as it was believed that this control strategy would be more economically

https://doi.org/10.5194/wes-2020-21
Preprint. Discussion started: 11 March 2020

viable than the alternative considered: partial pitch control of the blade. The ailerons were designed as plain hinged flaps extending from approx 60% to 99% of the chord.

A further full scale test of an active flap system is given in (Berg, 2014a) and (Berg, 2014b), where the 9m long CX-100 blade was retrofitted with active flaps integrated in the structure. For this purpose, a rigid hinged flap was incorporated in the trailing edge area of the original blade. The effective hinge area of the flap covered the aft 20% of the chord, of the outboard 20% of the blade span (approx. 2m of the blade). The flap was actuated with a motor embedded in the structure both in constant offsets as well as sinusoidal actuation.

Further full scale tests were performed by RISØ Laboratories in collaboration with Vestas Wind Systems A/S on a Vestas V27-225 kW turbine (13m blade length) equipped with a 70 cm long trailing edge flap as described by Castaignet (2010) and Castaignet (2013a). During this test, which spanned for several hours split among several days, the turbine load control with active flaps was ran in intervals of 2 minutes with, and 2 minutes without the flaps active. During 10 of these measurement intervals, an average blade root flapwise fatigue load reduction of 14% was achieved for a test running 38 minutes using a frequency weighted model predictive control. The controller strategy for this test is further discussed in Castaignet (2013b) and Couchman (2014).

The work described in the context of this paper consists of a full-scale long-term validation of two different revisions of an active flap system (described in the next section) on a SWT-4.0-130 turbine (blade length 63.4m). A numerical and experimental characterization of the first revision of the active flap component can be found in (Gomez, 2018). The main purpose of the test is to make an overall aerodynamic and load-wise performance characterization of the system and not to test any specific closed-loop control strategy. Furthermore, the tests presented herein were performed with the goal of characterizing an innovative solution, which in contrast to what has been done in the past, is tested in industrial full scale, during a long period, with remote control and surveillance, as well as with high quality data acquisition of both the turbine and inflow data.

2 Test description

The test setup consists of a SWT-4.0-130 turbine (63.4m blade length) retrofitted with the Active Flap System (AFS) on one of the blades. The turbine was equipped with a pressure supply system for the pneumatic activation of the AFS. All systems were designed to be activated remotely interfacing through the turbine communication unit. Two versions of the AFS were tested in independent campaigns as shown in figure 1. The two flap revisions used in phases 1 and 2 are referred to as FT008rev9 and FT008rev10, respectively. Test phase 2 was improved taking into account learnings from phase 1. During phase 2 of testing, besides upgrading the AFS to a newer, more aerodynamically and structural optimized geometry, an upgrade of the pressure supply system was performed focusing on increasing the air storage capacity of the system, as well as a new system allowing continuous variation of pressure levels (in contrast to phase 1, where only discrete levels are used) - see table 1 for reference. Therefore, the tests presented herein will focus mainly on test phase 2.

For the validation of the load impact of the AFS, the turbine was instrumented with strain gauges in the root of all three blades as well as at the tower top position. Per default, all operational parameters of the turbine such as pitch, rotor speed, and

https://doi.org/10.5194/wes-2020-21
Preprint. Discussion started: 11 March 2020

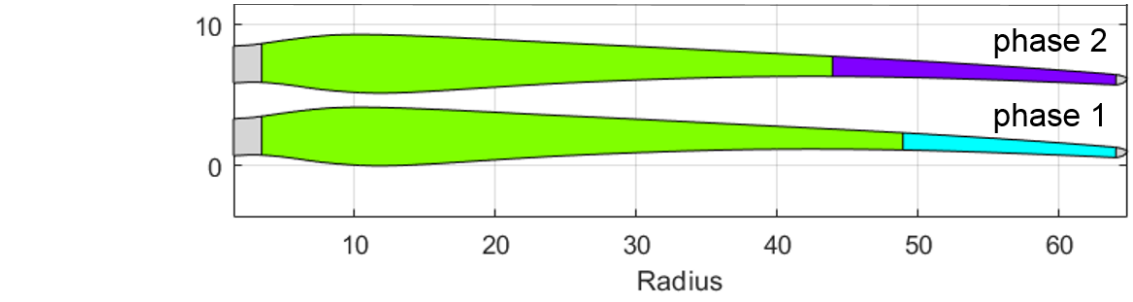

Figure 1. Blade layout of AFS

	Phase 1	**Phase 2**
Date	Oct 2017 - June 2018	Dec 2018 - June 2019
Turbine	SWT-4.0-130	SWT-4.0-130
AFS revision	FT008rev9	FT008rev10
AFS actuation	discrete positions	continuous angle variation
Actuation validation type	on-off cycles	on-off cycles
Location on blade	47.5 - 62.5 m	42.5 - 62.5 m

Table 1. Campaign information

power are continuously logged. The wind speed and direction, as well as atmospheric pressure, temperature, and humidity, are measured on a met-mast located 2.5D in front of the turbine. The wind speed and direction at 10 different heights throughout the full extension of the rotor are measured with a nearby Lidar in order to have a good assessment of shear and veer (see figure 2). The pressure level of the AFS, as well as the digital signals for activation of supply valves are logged synchronously with all other quantities. The pressure-deflection characteristic of the flap is known from previous wind tunnel measurements (Gomez, 2018). All quantities are logged continuously for the full measurement period with a sampling frequency of 25 Hz (except the lidar signals, which are sampled with 1 Hz). In addition, the blade is equipped with a remote surveillance camera in order to monitor the AFS (see exemplary view in figure 3a).

The primary characterization of the system is performed by actuating the flaps using pressure steps (equivalent to steps of flap deflection angles), cycling through different pressure levels over constant time intervals. Contrary to the work of Berg (2014a), where the cycles chosen were of 30s, or the work of Castaignet (2013a) with 2 minute cycles, the cycles chosen for the current work are 30 minutes long, allowing both to gather the high frequency transient response of the system, as well as three independent 10-min time stamps of statistical power and load values for every cycle. The cycles were performed during several months, cycling through different flap deflection levels, allowing therefore data acquisition over a very wide range of wind and operating conditions. During the measurement period, the AFS operated at wind speeds covering the range of approx. $2\frac{m}{s}$ to $15\frac{m}{s}$ for turbulence intensities between approx 3% and 30%.

https://doi.org/10.5194/wes-2020-21
Preprint. Discussion started: 11 March 2020

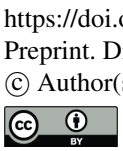

eawe european academy of wind energy
Open Access WIND ENERGY SCIENCE DISCUSSIONS

Figure 2. Test site layout. Map data taken from © GoogleMaps copyright - 2020

(a) Active flap seen from hub (b) View of flap activation

Figure 3. Views of AFS

The aerodynamic characteristics of the AFS operated at different pressure levels are known from previous wind tunnel measurements as described by Gomez (2018). An example of the measured normalized aerodynamic coefficients for the first revision of the AFS (FT008rev9) is shown in figure 4 (depicting the impact on lift coefficient and gliding ratio of the airfoil). The curve labeled as *baseline* represents the airfoil without AFS.

3 Results

This chapter gives a summary of results obtained for both field test campaigns of the AFS. For both campaigns, a series of activation tests were performed to ensure the correct functionality of the system. Visual checks were also performed in order to verify the flap is deflecting properly and is not blocked or restrained in any way.

https://doi.org/10.5194/wes-2020-21
Preprint. Discussion started: 11 March 2020

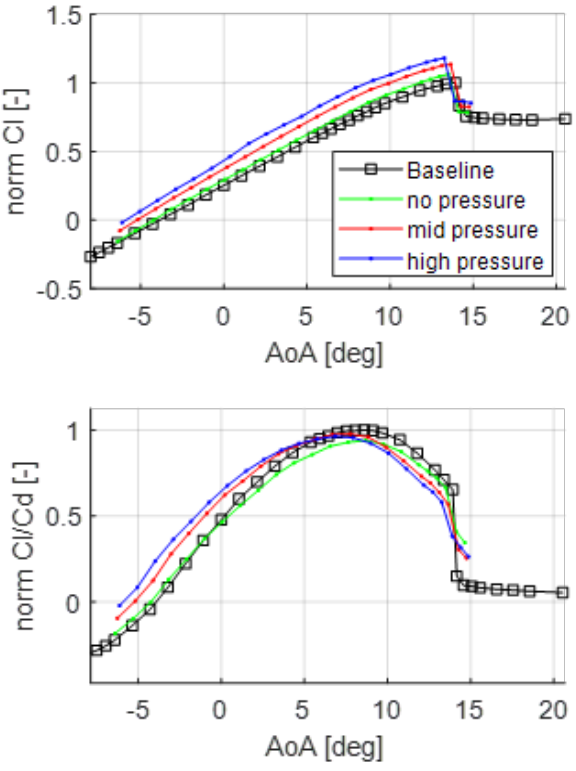

Figure 4. Exemplary normalized aerodynamic coefficients for FT008-rev9 AFS

Due to the stochastic nature of the measurements (with varying levels of inflow turbulence, shear, etc.), the comparison of results as a function of wind speed is not the best choice. Measured variables as a function of wind speed normally have high scatter due to atmospheric variability, but also due to the coherence effects between the measurement point of the undisturbed wind speed (the met mast), and the location of the turbine. Due to this, a new method for analysis is developed, consisting of a blade-to-blade load variation representation. For this purpose, neighboring blades are used for the analysis based on flapwise bending moment measurements via strain gauges placed at the root of the blades. Utilizing this method, the uncertainty related to inflow conditions as well as to coherence in the wind field is removed to a large extent. In what follows, a brief description of the method is given.

3.1 Blade to blade analysis

The blade-to-blade analysis method (referred to as b2b-method in what follows) consists mainly of two independent types of analysis: a time averaged, and a transient analysis.

https://doi.org/10.5194/wes-2020-21
Preprint. Discussion started: 11 March 2020

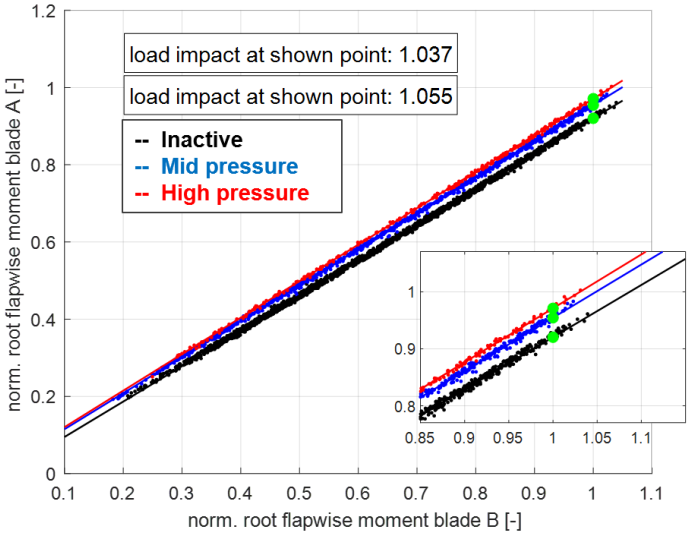

Figure 5. Example of a time averaged blade to blade load comparison

The *time averaged analysis* is quite straight forward and requires only a turbine equipped with a calibrated means of measuring bending moments. A standard method for this consists on the calibration of strain measurements in the root area of the blade, where strain gauges are placed on the intersection points between the contour of the blade and the principal axes of the section. With independent strain measurements of two different blades (and the corresponding transfer function to obtain bending moments), the integral load impact of an active device on a blade can be readily measured. One of the blades of the turbine is equipped with the active device in question, whilst the other two blades are left unchanged. In this fashion, the two unchanged blades serve as reference for comparison. This type of comparison between the blade retrofitted with the AFS and the baseline blades has quite low scatter, as both blades are seeing all the time the same time averaged impact of shear, turbulence, veer, and turbine dynamics. Avoiding the use of wind speed measurements increases greatly the correlation of the measured signals because there is no dependence on the coherence of the turbulent wind field. Furthermore, the uncertainty related to point-wise wind speed measurements is removed. A similar method has been previously used by Bak (2016) to evaluate the impact of vortex generators on a full scale wind turbine. An example of such b2b comparison between the blade equipped with the AFS and a reference blade is shown in figure 5, where normalized flapwise bending moments are shown for blades A and B for three different pressure levels for the AFS.

The purpose of the *transient analysis* part of the b2b-method is to extract the transient response (in this case, the step response) of the system as it undergoes changes in time. The complexity of measuring the transient aerodynamic response lies in the fact that this type of high frequency response will normally be hidden in the dynamics of the blades responding to turbulence, vibrations, rotation, etc. The core of the transient analysis of the b2b-method relies on the elimination of the

https://doi.org/10.5194/wes-2020-21
Preprint. Discussion started: 11 March 2020

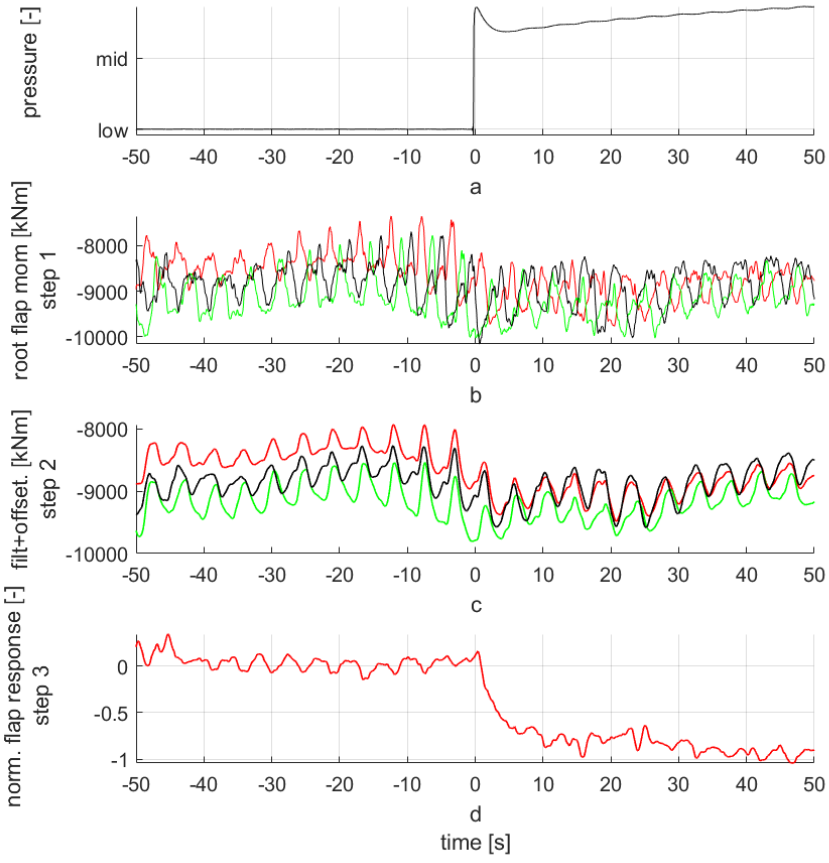

Figure 6. Transient signal analysis

periodic signal dynamics due to rotation and forced vibrations via an artificial time-shift of signals of neighboring blades, together with the elimination of the dynamics due to turbulence via time filtering and ensemble averaging.

The *first step* of the transient b2b-method is to read the bending moment signals from all three blades (the blade retrofitted with the AFS, and the remaining two blades as reference) a sufficient amount of time before and after the dynamic change of the system (e.g. a pressure step of the AFS). Such signals are shown exemplary in figure 6b.

The *second step* consists on a low-pass filtering of all signals with an appropriate time constant and a subsequent time shift. In the current analysis, all signals were filtered using a low-pass first order filter with a $1s$ time constant. The time constant must not be too large, else it has an impact on the dynamics due to the natural phase-shift effect of the filter, and should not be too small else there will be a large amount of high frequency cycles which will still be visible after the ensemble averaging. The leading and trailing baseline blades are shifted backwards and forward in time, respectively, by $\Delta t = \pm\frac{2\pi}{3\bar{\Omega}}$, where $\bar{\Omega}$ is the

https://doi.org/10.5194/wes-2020-21
Preprint. Discussion started: 11 March 2020

eawe european academy of wind energy
Open Access WIND ENERGY SCIENCE DISCUSSIONS

average rotor speed expressed in rad/s during the respective period. The output of this step is shown exemplary in figure 6c, where in contrast to figure 6b, the signals are now clean of high frequency content and have peaks aligned in time.

The *third step* of the method is to detect the point in time where the dynamic change of the system takes place, and to time-shift the signals such that this time corresponds with $t = 0$ (see example in figure 6a). This will be important for the next step (the ensemble averaging). For the current work, the controller actuation signal of the supply valve of the system was read directly, knowing then precisely the starting time of the transient response. At this stage, the bending moments of both reference blades are averaged. This average reference value is then subtracted from the bending moment signal of the blade equipped with AFS, and this differential load is normalized based on the amplitude of the load step, leading thus to the normalized impact on loading from this single blade. An example of the result of this stage of the signal processing is shown in figure 6d.

The *fourth and last step* of the transient response extraction is the ensemble averaging of these delta loads across several actuations, such that the stochastic variations are averaged out (e.g. variations due to turbulence). This is shown in the results section in figure 8.

3.2 Field measurements

The first section of results relates to the steady load impact of the AFS used in phase 1 and phase 2 of the field test. The relation between the flapwise blade root bending moment and wind speed is not monotonic. For modern pitch controlled turbines, the flapwise moment will increase with wind speed until it reaches a maximum close to the region of rated power and in this region the angle of attack (AoA) variations as a function of wind speed are small. Subsequently, the flapwise bending moment will decrease as wind speed further increases, and the AoA of the blade sections will decrease as the blade pitches into the wind. Due to this non-monotonic behavior of the bending moment and the related changes in AoA, it is important to differentiate between regions of low and high wind when doing the time averaged analysis. For the measurements referred to here, the data sets were divided into measurement points with 10-min average wind speed below and above $9\frac{m}{s}$, respectively.

All 10-min bins during the measurement periods of phase 1 and 2 were collected and split into low and high wind areas. For this data set, the b2b comparison between blade A (equipped with the AFS) and blade B (one of the baseline blades) is shown in figure 7. There is a high correlation between these bending moment measurements (seen by the linear relation and the very low scatter of the plot). Furthermore, the data is filtered based on two different pressure levels representing the operation envelope of the active flap system. The impact of the active system is seen in the fact that two clearly defined lines are seen in these plots. The relative change of loading of blade A vs. blade B at different locations along these lines represents the impact of loading measured at the blade root for different wind speeds. The load levels have been normalized for clarity, where the normalization factor has been chosen as the average peak loading of the bending moment vs. wind speed curve. Therefore, values close to 1 in figure 7 represent peak loading of the turbine and are representative of the maximum loading level of the turbine (corresponding to wind speeds close to $9\frac{m}{s}$). For very high operational wind speeds (for example $15\frac{m}{s}$ and above), the bending moment will decrease as already discussed. For this wind speed range, a representative normalized load value of 0.66

https://doi.org/10.5194/wes-2020-21
Preprint. Discussion started: 11 March 2020

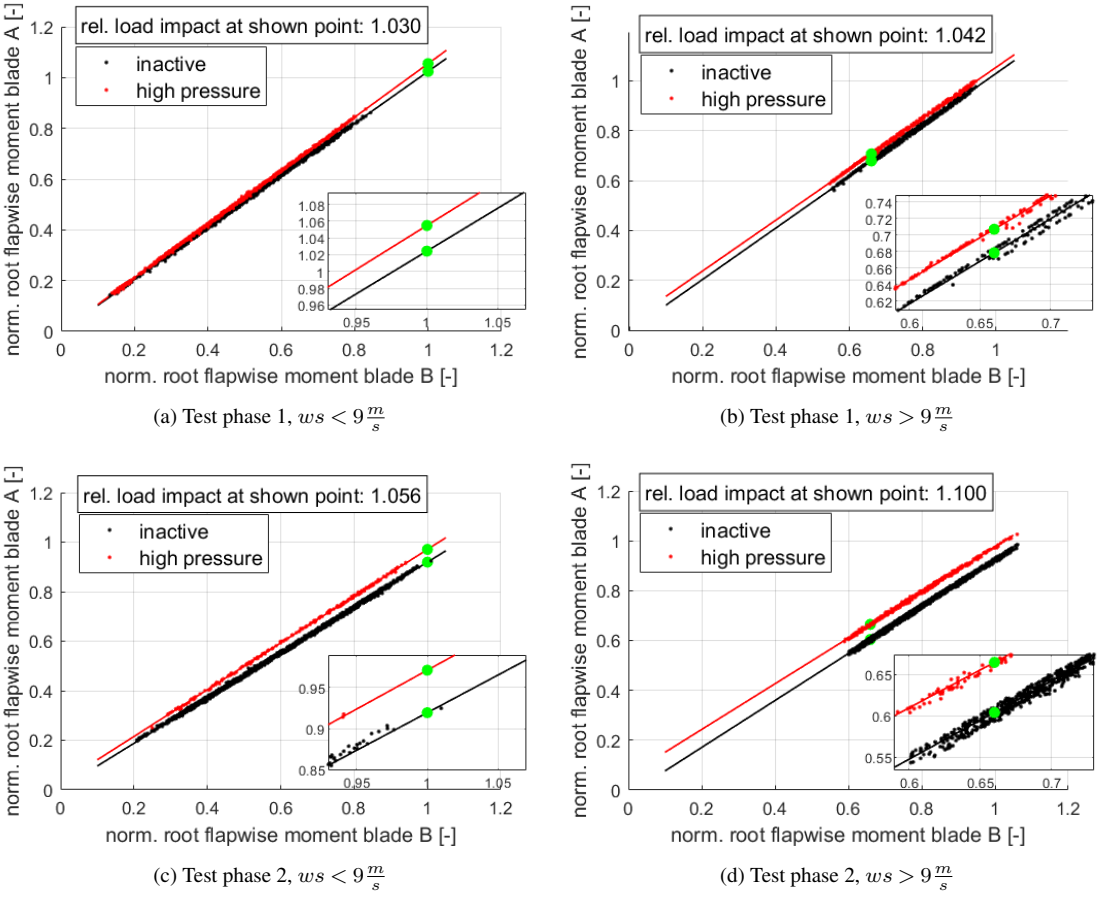

(a) Test phase 1, $ws < 9\frac{m}{s}$

(b) Test phase 1, $ws > 9\frac{m}{s}$

(c) Test phase 2, $ws < 9\frac{m}{s}$

(d) Test phase 2, $ws > 9\frac{m}{s}$

Figure 7. Time averaged load response for AFS during phase 1 and 2 of field test

is chosen. These two values (1 and 0.66), representative of peak loading and high wind speed loading, respectively, can be seen highlighted in figure 7 together with the corresponding load ratio.

It can be seen that for phase 1, the load impact at the load root is measured to be in the range between 3% and 4.2%, whereas for the phase 2, the loading ratio increases up to approx. 5.6% to 10%. It is worth mentioning that the load ratios for outboard locations of the blade which are closer to the AFS will be larger, but these values were not measured during this field test. The load handle of 5% to 10% obtained in phase 2 is one of the major results of the project, highlighting the potential of the AFS to manipulate actively the loads of the turbine.

For the transient analysis of the data accumulated during the field test, the different changes in pressure of the AFS were categorized depending on the start and end value of the pressure level. The data presented herein is given for so-called type H1 and type L2 pressure steps. Type H1 represents a step change in pressure from the lowest to the highest threshold of the system, whereas a type L2 step represents a step change from the highest towards the lowest pressure thresholds. This means in other words that type H1 represent a full activation of the AFS, and type L2 the deactivation. These two type of pressure

https://doi.org/10.5194/wes-2020-21
Preprint. Discussion started: 11 March 2020

eawe european academy of wind energy
Open Access WIND ENERGY SCIENCE DISCUSSIONS

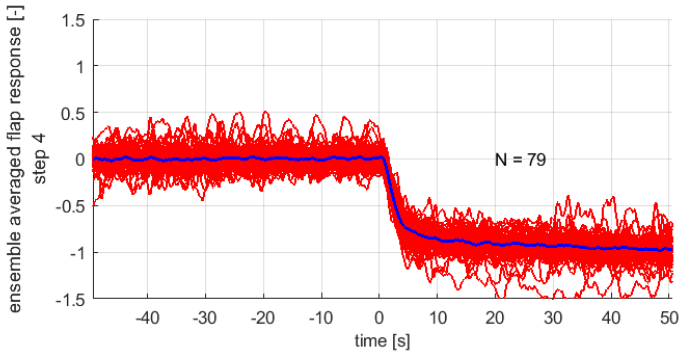

(a) Pressure step type H1

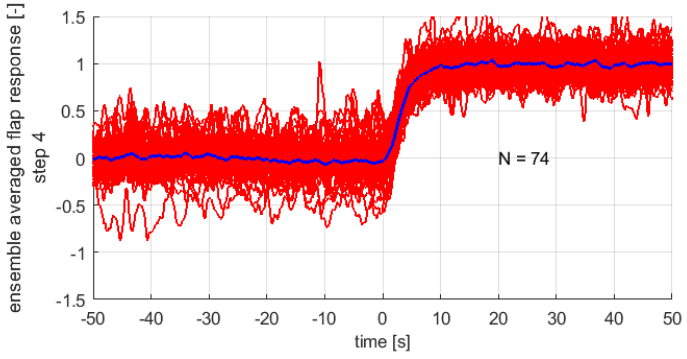

(b) Pressure step type L2

Figure 8. Transient analysis for pressure steps of type H1 and L2

jumps show different dynamic behavior due to the differences in flow dynamics during the inflation and deflation of the AFS. The ensemble averaged response of the H1 and L2 pressure steps are depicted in figure 8. For the analysis shown, the number of individual time series analyzed is given in the plot with the value N. Every dynamic step is extracted at the end / beginning of one of the 30 minute intervals described earlier.

The pressure response measurement of the transient analysis must be used with care due to the physical distance between the location of the actual measurement, and the location of the AFS. The pressure is measured directly at the exit supply valve. This pressure signal is used for filtering the measurements according to the pressure level, but not for the dynamic analysis as it does not represent accurately the instantaneous pressure at the AFS location (due to the flow dynamics in the pressure supply line). The pressure level at the location of the AFS was not measured in these test campaigns due to the long-term duration of the measurements to avoid interference with the lightning protection system. Nevertheless, with the pressure transient at the supply valve location during the activation sequence, it can be seen that the air supply to the AFS reaches saturation (this can be seen from the slow increase in pressure) and will be addressed in future developments.

https://doi.org/10.5194/wes-2020-21
Preprint. Discussion started: 11 March 2020

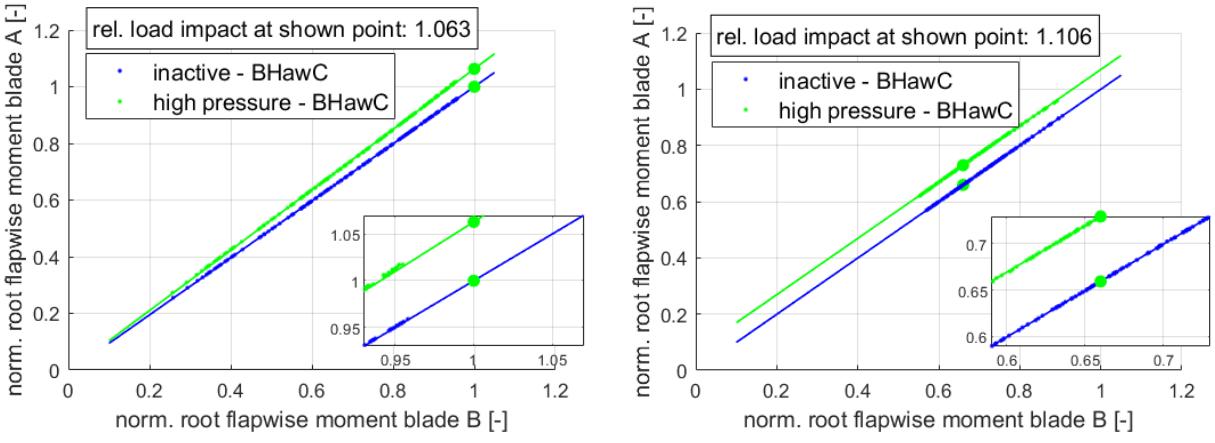

(a) Phase 2 simulations at low wind

(b) Phase 2 simulations at high wind

Figure 9. Aeroelastic simulations corresponding to phase 2 of the test at low and high wind regimes

3.3 Aeroelastic simulations

Aeroelastic simulations are performed with SiemensGamesa's in-house solver BHawC (Rubak (2005); Fisker (2011)). The simulations are performed in a so-called one-to-one fashion (o2o) (see Enevoldsen (2018) for reference). The o2o calculations are high fidelity aeroelastic simulations performed in a *digital twin* manner, meaning that the structural model is matched exactly to the particular turbine under consideration both in geometry, structural description, and system dynamics, but also where every single 10 min atmospheric inflow measurement point is recreated numerically. The aerodynamic input to the simulation in form of airfoil polars is taken directly from wind tunnel measurements of the AFS. For the full period of phase 1 and phase 2 of the field test there exists therefore the same corresponding period of o2o equivalent aeroleastic simulations. The input to the simulations is dependent on good inflow measurements and therefore only the wind sector where the metmast / lidar is unaffected by the wake of any turbine of the park is used for comparison. For this reason, even though the b2b method is generic for the whole range of directions, only the west sector is taken in consideration for o2o simulations ($270 \pm 30 deg$).

The simulations results presented here focus on phase 2 of the measurement with AFS FT008rev10. In figure 9, the time-averaged b2b results for the blade equipped with AFS and a baseline blade are shown. These results, similarly as for the experimental results, are shown for low wind and high wind regimes below and above $9\frac{m}{s}$, respectively. As can be seen from the figure, the aeroelastic simulations are in very good agreement with measurements, predicting a load impact of 6.3% representative for peak loading, compared to the measured 5.6%, and 10.6% compared to the measured 10.0% representative for high wind situations (cp. figure 7).

https://doi.org/10.5194/wes-2020-21
Preprint. Discussion started: 11 March 2020

eawe european academy of wind energy
Open Access WIND ENERGY SCIENCE DISCUSSIONS

4 Conclusions

Two independent long term validation campaigns were conducted for a pneumatic active flap system on a full scale wind turbine. The AFS was actuated in an on-off fashion in order to assess the load impact of the system. The first revision of the AFS was activated at discretely varying pressure levels and showed a potential load impact between 3-4% for root flapwise bending moments. In a second phase of the testing campaign, the AFS was optimized both aerodynamically and structurally, in combination with an upgrade of the pressure supply system which enabled continuously varying angle activation. This revision of the AFS showed a potential load impact between 5-10% at the root of the blade.

The measurements performed were accompanied with high fidelity aeroelastic simulations where the aerodynamic input was based on polars measured in a wind tunnel, and the atmospheric inflow was based on metmast and lidar measurements. Very good agreement was found between the measurements and the simulation results.

The AFS was shown to operate in a robust way and without major drawbacks. The AFS revisions were tested independently for over 6 months each, covering therefore a wide range of wind speeds, temperatures, and atmospheric conditions. The loads of the turbine were measured as well in a robust and accurate manner, enabling a good estimate of the potential load impact levels of the AFS. Finally, a novel method was developed in order to directly measure the transient behavior of the AFS in a highly time varying environment.

Author contributions. All authors contributed significantly to the work presented within this paper.

Competing interests. The authors declare they have no competing interests.

Acknowledgements. The work presented in this article is part of the Induflap2 project (Induflap2) which is a research and development project carried out in the period from 2015 to 2019. The authors wish to acknowledge EUDP for the funding given to the project (journal nr. 64015-0069).

https://doi.org/10.5194/wes-2020-21
Preprint. Discussion started: 11 March 2020

eawe european academy of wind energy
Open Access WIND ENERGY SCIENCE DISCUSSIONS

References

Bak, C., Skrzypinski, W., Gaunaa, M., Villanueva, H., Brønnum, N.F., and Kruse, E.K.: Full scale wind turbine test of vortex generators mounted on the entire blade, J. Phys.: Conf. Ser., 753-022001, 2016.

Barlas, T.K. and van Kuik, G.A.M: Review of state of the art in smart rotor control research for wind turbines Progress in Aerospace Sciences, vol. 46, 1–27, 2010.

Berg, J., Resor, B.R., Paquette, J.A., and White, J.: SMART wind turbine rotor: design and field test, Sandia National Laboratories, Wind Energy Technologies Department, SAND2014-0681, Albuquerque, USA, 2014.

Berg, J., 2014, Barone, M.F., and Yoder, N.C.: SMART wind turbine rotor: data analysis and conclusions Sandia National Laboratories, Wind Energy Technologies Department, SAND2014-0712, Albuquerque, USA, 2014.

Castaignet, D., Barlas, T.K., Buhl, T., Poulsen, N.K., Wedel-Heinen, J.J., Olesen, N.A., Bak, C., and Kim, T.: Full-scale test of trailing edge flaps on a Vestas V27 wind turbine: active load reduction and system identification, Journal of Wind Energy, DOI 10.1002/we.1589, 2013.

Castaignet, D., Couchman, I., Poulsen, N.K., Buhl, T., and Wedel-Heinen, J.J.: Frequency weighted model predictive control of trailing edge flaps on a wind turbine blade, IEEE Transactions On Control Systems Technology, vol.21 No. 4 1105-1116, 2013.

Castaignet, D., Wedel-Heinen, J., Kim, T., Buhl, T., and Poulsen, N.: Results from the first full scale wind turbine equipped with trailing edge flaps, Proceedings of the 28th AIAA Applied Aerodynamics Conference, AIAA 10.2514/6.2010-4407, Chicago, USA, 2010.

Couchman, I., Castaignet, D., Poulsen, N.K., Buhl, T., Wedel-Heinen, J.K., and Olesen, N.A.: Active load reduction by means of trailing edge flaps on a wind turbine blade, American Control Conference June 4-6, 2014, Portland, Oregon, USA, 2014.

Enevoldsen, P.B.: Load validation and advanced modelling, Advances in Rotor Blades for Wind Turbines - IQPC Conference, April 24-26 2014. Bremen, Germany, 2014.

Energiteknologiske Udviklings-. of Demonstrationsprogram. Project Journal Nr. 64015-0069.

Skjoldan, P.F.: Aeroelastic modal dynamics of wind turbines including anisotropic effects. Ph.D. Thesis, DTU Risoe-PhD-66, 2011.

General Electric Company: MOD-5A Wind turbine generator program design report. Volume 1 - Executive Summary, NASA CR-174734, Cleveland, USA, 1984.

Gomez, A., Enevoldsen, P.B., Akay, B., Barlas, T.K., Fischer, A., and Madsen, H.Aa.: Experimental and numerical validation of active flaps for wind turbine blades, J. Phys.: Conf. Ser. 1037-022039, DOI :10.1088/1742-6596/1037/2/022039, 2018.

Induflap2 project information website. http://www.infuflap.dk, last access: Feb 3, 2020.

Johnson, S. and van Dam, C.P.: Active load control techniques for wind turbines, Sandia National Laboratories, SAND2008-4809, Dept of mech. and aeronautical engineering. University of California. Davis, USA, 2008.

Pechlivanoglou, G.: Passive and active flow control solutions for wind turbine blades. Ph.D. Thesis, Technische Universität Berlin, 2013.

Rubak R. and Petersen, J.T.: Monopile as Part of Aeroelastic Wind Turbine Simulation Code, Proceedings of Copenhagen Offshore Wind 2005.